Respiratory Physiology & Neurobiology 280 (2020) 103482

Contents lists available at ScienceDirect

Respiratory Physiology & Neurobiology

journal homepage: www.elsevier.com/locate/resphysiol

Activation of μ-opioid receptors differentially affects the preBötzinger Complex and neighbouring regions of the respiratory network in the adult rabbit

Elenia Cinelli*, Fulvia Bongianni, Tito Pantaleo, Donatella Mutolo

Dipartimento di Medicina Sperimentale e Clinica, Sezione Scienze Fisiologiche, Università degli Studi di Firenze, Viale G.B. Morgagni 63, 50134, Firenze, Italy

ARTICLE INFO

Keywords:
Opioid-induced respiratory depression
μ-Opioid receptors
preBötzinger Complex
Medullary respiratory network
Control of breathing

ABSTRACT

The role of the different components of the respiratory network in the mediation of opioid-induced respiratory depression is still unclear. We investigated the contribution of the preBötzinger Complex (preBötC) and the neighbouring Bötzinger Complex (BötC) and inspiratory portion of the ventral respiratory group (iVRG) in anesthetized, vagotomized, paralyzed and artificially ventilated adult rabbits making use of bilateral microinjections (30 − 50 nl) of the μ-opioid receptor agonist [D-Ala^2, N-Me-Phe^4, Gly^5-ol]-enkephalin (DAMGO). Dose-dependent effects were observed. In the preBötC and the BötC 0.1 mM DAMGO microinjections caused mainly reductions in peak phrenic amplitude associated with tonic phrenic activity and irregular (ataxic) patterns of breathing that were more pronounced in the preBötC. Apneic effects developed at 0.5 mM. In the iVRG DAMGO provoked decreases in amplitude and frequency of phrenic bursts at 0.1 mM and apnea at 0.5 mM. Local 5 mM naloxone reversed the apneic effects. The results imply that different components of the respiratory network may contribute to opioid-induced respiratory disorders.

1. Introduction

It is well known that opioid overdose exerts potent depressant and potentially fatal effects on respiration by activating μ-opioid receptors (MORs; e.g. Pattinson, 2008; Dahan et al., 2010). Nevertheless, opioid agonists acting on MORs are usually prescribed to relief pain due to their powerful analgesic effects (Yaksh et al., 2015). The risk of opioid-induced death appears to be correlated with progressive irregularities in the breathing pattern rather than only with severe decreases in respiratory rate leading to apnea (Bouillon et al., 2003; Pattinson, 2008). The medullary preBötzinger Complex (preBötC) has been the first region of the respiratory network to be considered crucial for inducing opioid-related respiratory depression (Gray et al., 1999; Lalley, 2003; Montandon et al., 2011, 2016; Montandon and Horner, 2014; Qi et al., 2017). This region plays an essential role in inspiratory rhythm generation. A subpopulation of glutamatergic neurons of the preBötC characterized by the expression of neurokinin-1 receptors (NK1Rs) contains MORs (Smith et al., 1991; Gray et al., 1999, 2001; Feldman et al., 2003; McKay et al., 2005; Tan et al., 2008; Del Negro et al., 2018). Of note, it has been found that the activation of MORs within the preBötC of medullary slices from neonatal mice (see Sun et al., 2019 also for further Refs.) causes an inhibitory modulation of inspiratory rhythmic activity by acting on burstlet-producing Dbx1-derived neurons, an important glutamatergic subpopulation on which appears to rely the process driving respiratory rhythmogenesis. Consistently, such opioid-induced modulation is abolished in mice with genetic deletion of MORs within this preBötC subpopulation. However, the role of the preBötC in the opioid-induced respiratory depression has been heavily questioned, at least in adult animals (Lonergan et al., 2003; Mustapic et al., 2010; Prkic et al., 2012; Stucke et al., 2015; Miller et al., 2017). In more detail, the attention has been focused on the pontine respiratory region. It has been reported that in both dogs and rabbits the medial parabrachial nucleus mediates part of the opioid-induced respiratory depression (Prkic et al., 2012; Miller et al., 2017). Furthermore, recent findings (Levitt et al., 2015; Varga et al., 2020) strongly suggest that the Kölliker-Fuse (KF) nucleus contributes to opioid-induced respiratory disturbances, including respiratory depression and impairment of the upper airway function, consistently with the primary role of KF neurons in rate stabilization, upper airway patency and post-inspiratory activity generation (e.g. Lumsden, 1923; St-John and Paton, 2004; Dutschmann and Herbert, 2006; Smith et al., 2007; Dutschmann and Dick, 2012). Interestingly, Varga et al. (2020) using a conditional genetic knockout approach in awake adult mice have shown that preBötC neurons and, to a larger extent, KF neurons contribute to the

* Corresponding author.
E-mail address: elenia.cinelli@unifi.it (E. Cinelli).

https://doi.org/10.1016/j.resp.2020.103482
Received 16 March 2020; Received in revised form 5 June 2020; Accepted 12 June 2020
Available online 15 June 2020
1569-9048/

MOR-induced respiratory depression. They conclude that opioids differentially affect distributed key areas of the respiratory network and that more than one of them has a role in the genesis of respiratory disorders. In this context, it should be mentioned that evidence has been provided in the mouse that a medullary neural network, named post-inspiratory complex, generates post-inspiratory activity and is highly responsive to the activation of MORs (Anderson et al., 2016; Anderson and Ramirez, 2017). However, Toor et al. (2019) have recently provided data showing that the intermediate reticular nucleus of the rat, that corresponds well neuroanatomically and phenotypically to the mouse post-inspiratory complex, contributes to the post-inspiratory activity, but is not required for termination of inspiration or recruitment of post-inspiratory activity during acute hypoxemia. They suggested that this neuronal population may not represent a distinct central pattern generator for post-inspiratory activity, but instead may operate as a relay that distributes post-inspiratory activity generated elsewhere.

Although MORs are expressed throughout the entire brainstem respiratory network (e.g. Mansour et al., 1994; Lonergan et al., 2003; Zhang et al., 2007, 2011), no information is available on the effects of their activation within some very important regions of the medullary respiratory network. Thus, the present study was undertaken to investigate the contribution of the preBötC and the neighbouring Bötzinger Complex (BötC) and inspiratory portion of the ventral respiratory group (iVRG) to the MOR-induced respiratory depression. Experiments were carried out on anesthetized, vagotomized, paralyzed and artificially ventilated adult rabbits making use of microinjections of the MOR agonist [D-Ala^2, N-Me-Phe^4, Gly^5-ol]-enkephalin (DAMGO).

2. Materials and methods

2.1. Ethical approval

Experiments were carried out on 15 male New Zealand white rabbits (2.8–3.4 kg) purchased from the Pampaloni Farm and Laboratory Animal Co. (Fauglia, Pisa, Italy). Rabbits were maintained on a 12-h light/12-h dark cycle with food and water *ad libitum*. All animal care and experimental procedures were conducted in accordance with the Italian legislation and the official regulations of the European Community Council on the use of laboratory animals (Decreto Legislativo 4/3/2014 no. 26 and directive 2010/63/UE). The study was approved by the Animal Care and Use Committee of the University of Florence. All efforts were made to minimize animal suffering and to reduce the number of animals used. At the end of the experiment the animal was euthanized with an overdose of anesthetic.

2.2. Animal preparation

Experimental procedures and details on the methods employed have previously been fully described (Bongianni et al., 1997, 2002, 2008, 2010; Mutolo et al., 2002, 2005; Pantaleo et al., 2011; Iovino et al., 2019). The animals were anesthetized (ear marginal vein) with a mixture of α-chloralose (40 mg/kg i.v.; Sigma-Aldrich, St. Louis, MO, USA) and urethane (800 mg/kg i.v.; Sigma-Aldrich), supplemented (femoral vein) when necessary (4 mg/kg and 80 mg/kg, respectively). The adequacy of anesthesia was assessed by the absence of reflex withdrawal of the hindlimb in response to noxious pinching of the hindpaw. After cannulation of the trachea, polyethylene catheters were inserted into a femoral artery and vein for monitoring arterial blood pressure and for drug administration, respectively. Both C5 phrenic roots were dissected free, cut distally and prepared for recordings. Both cervical vagus nerves were separated from the sympathetic trunks for subsequent vagotomy. The animal was placed in a prone position and fixed in a stereotaxic instrument by a stereotaxic head holder and vertebral clamps (Baltimore Instrument, Baltimore, MA, USA); the head was ventroflexed to facilitate recordings from the medulla. The dorsal surface of the medulla was widely exposed by occipital craniotomy, and the dura and arachnoid membranes were removed. The posterior part of the cerebellum was removed by gentle suction to provide access to the rostral part of the medulla. All exposed tissues were covered with warm paraffin oil (~38 °C). Body temperature was maintained at 38.5 – 39 °C by a heating blanket controlled by a rectal thermistor probe. The animals were vagotomized, paralyzed (gallamine triethiodide 4 mg/kg i.v., supplemented with 2 mg/kg every 30 min; Sigma-Aldrich) and artificially ventilated. In paralyzed animals, the depth of anesthesia was assessed by ascertaining the presence of a stable and regular pattern of phrenic nerve activity as well as the absence of fluctuations in arterial blood pressure whether spontaneous or in response to somatic nociceptive stimulation. End-tidal CO_2 partial pressure was maintained approximately at the level of spontaneous breathing (28.5 – 32 mmHg) by adjusting the frequency and stroke volume of the respiratory pump.

2.3. Recording procedures

Efferent phrenic nerve activity was recorded with bipolar platinum electrodes from desheathed C5 phrenic roots, amplified, full-wave rectified and passed through a leaky integrator (low-pass RC filter, time constant 100 ms) to obtain a 'moving average' of the activity, usually referred to in the literature as 'integrated' activity. Recording conditions were maintained constant throughout each experiment. Extracellular recordings from medullary neurons were made with tungsten microelectrodes (5 – 10 MΩ impedance as tested at 1 kHz). The most rostral extent of the area postrema on the midline was defined as the obex and used as a standard point of anatomic reference. Neuronal activity (see Fig. 5A) was recorded from rostral expiratory neurons of the BötC (3.0–4.5 mm rostral to the obex, 2.4–3.2 mm lateral to the midline and 3.5–4.6 mm below the dorsal medullary surface), from the inspiratory neurons of the iVRG (from 0.7 caudal to 2.0 mm rostral to the obex, 2.3–3.2 mm lateral to the midline and 3.0–3.5 mm below the dorsal medullary face) and from the transition zone between the BötC and the iVRG where a mix of inspiratory and expiratory neurons is present (2.1–2.9 mm rostral to the obex, 2.4–3.2 mm lateral to the midline and 3.5–4.2 mm below the dorsal medullary surface). The latter region has already been extensively investigated in the rabbit with lesion and neuropharmacological approaches (Mutolo et al., 2002, 2005; Bongianni et al., 2008, 2010; Pantaleo et al., 2011; Stucke et al., 2015; Iovino et al., 2019) and corresponds to the preBötC described in adult cats and rats (see e.g. Connelly et al., 1992; Schwarzacher et al., 1995; Rekling and Feldman, 1998; Solomon et al., 1999; Feldman and Del Negro, 2006; Feldman et al., 2013; Del Negro et al., 2018). A strain-gauge manometer was used for monitoring arterial blood pressure. End-tidal CO_2 partial pressure was monitored by an infrared CO_2 analyzer (Capnocheck Plus, Smiths Medical PM, Waukesha, WI, USA). Cardiorespiratory variables were acquired and analyzed by using a personal computer equipped with an analog-to-digital interface (Digidata 1440, Molecular Devices, Sunnyvale, CA, USA) and appropriate software (Axoscope, Molecular Devices). Integrated phrenic nerve activity as well as the signals of all studied variables were also recorded on an eight-channel rectilinearly writing chart recorder (model 8K20; NEC San-ei, Tokyo, Japan).

2.4. Microinjection procedures and experimental protocol

Bilateral microinjections were performed into the BötC, preBötC and the iVRG regions. Injection sites were localized by stereotaxic coordinates well known from previous studies (e.g. Bongianni et al., 2002, 2008, 2010; Mutolo et al., 2002, 2005; Iovino et al., 2019) as well as by extracellular recordings of neuronal activity with patterns of discharge characteristic of each investigated region (see Fig. 5A). In each experiment, the first step was to record neuronal activity. Then, preBötC localization was ascertained on each side of the medulla (see Fig. 5B

and C) by the presence of excitatory respiratory responses to microinjections (30 − 50 nl) of 20 mM D,L-homocysteic acid (DLH, 600 − 1000 pmol; Sigma-Aldrich), a broad-spectrum excitatory amino acid (EAA) agonist, that are widely considered a functional marker of this region in various animal models (e.g. Solomon et al., 1999; Wang et al., 2002; Monnier et al., 2003; Krolo et al., 2005; Mutolo et al., 2005; Bongianni et al., 2008, 2010; Radocaj et al., 2015; Stucke et al., 2015; Iovino et al., 2019). Subsequently, bilateral DAMGO microinjections were performed in one of the three medullary respiratory regions. This procedure helped us to adequately space micropipette penetrations and to place micropipette tip into the BötC or the iVRG sufficiently far (≥ 1.0 mm) from the preBötC region (for the spread of the injectate see below).

Bilateral microinjections (30 − 50 nl) were performed in succession using a single glass micropipette (tip diameter 10 − 25 μm) by applying pressure using an air-filled syringe connected to the micropipette by polyethylene tubing. The volume of the injectate was measured directly by monitoring the movement of the fluid meniscus in the pipette barrel with a dissecting microscope equipped with a fine reticule. The duration of each injection ranged from 5 to 10 s. Control injections of equal volumes of the vehicle solution at the responsive sites were also made in some occasions (two trials for each investigated region) before 0.1 mM DAMGO. Relatively small volumes of drug solutions were microinjected to restrict the spread of the injectate. Note that a volume of 50 nl should spread less than 400 μm in any direction from the injection site, according to our previous histological observations on the spread of injectates ≤ 50 nl (Mutolo et al., 2002, 2005) and to theoretical calculations by Nicholson (1985). Of note, relatively high concentrations of neuroactive drugs are required to achieve pharmacological effects in microinjection studies in *in vivo* preparations probably due to several complex factors that drastically reduce the actual drug concentration at the level of neurons located within the injected area. These factors include the large dilution volume constituted by the extracellular space and, possibly, the continuous washout by water and solute movements across the capillary walls. For an extensive discussion on the microinjection procedures see also Lipski et al., 1988; Nicholson and Sykova, 1998; Bongianni et al., 1997, 2002, 2008, 2010, Iovino et al., 2019. In two experiments, preBötC injection sites were marked by injecting green fluorescent latex microspheres (LumaFluor, New City, NY, USA) added to the 0.5 mM DAMGO solution. The following drugs were used: 20 mM DLH, 0.1 and 0.5 mM DAMGO (a μ-opioid receptor agonist; Sigma-Aldrich) and 5 mM naloxone (a largely prevailing μ-opioid receptor antagonist; Sigma-Aldrich). Drugs were dissolved in 0.9 % NaCl solution. The pH of the solutions was adjusted to 7.4 using either 0.1 N NaOH or 0.1 N HCl. The two DAMGO concentrations were tested in the same preparations. We waited for full recovery after the first injections and, in addition, we scheduled a time lag ≥ 30 min to avoid as much as possible receptor desensitization (see e.g. Dang and Christie, 2012). Drug concentrations were selected in preliminary trials. They were in the same range previously used in *in vivo* preparations (Mutolo et al., 2008, 2010; Mustapic et al., 2010; Stucke et al., 2015; Qi et al., 2017).

2.5. Histology

At the end of the experiments in which fluorescent microspheres were injected, the brain was perfused via a carotid artery with 0.9 % NaCl solution and then with 10 % formalin solution. After at least a 48-h immersion in 10 % formalin solution, the brain was placed in a hypertonic sucrose solution. Frozen 20-μm coronal sections stained with Cresyl violet were used for the histological control of injection sites. Coronal sections of the medulla were examined by a light and epifluorescence microscope (Eclipse E400, Nikon, Japan) equipped with the Nikon Intensiligh C-HGFI mercury-fibre illuminator. A Nikon DS-Fi1 digital camera was used to take photomicrographs. Illustration were prepared in Adobe Photoshop CS3 (Adobe Systems Incorporated). The atlas of Shek et al. (1986) was used for comparison.

2.6. Data collection and statistical analysis

We measured the total duration of the respiratory cycle (T_T) as well as the inspiratory (T_I) and expiratory (T_E) times. The respiratory frequency (breaths/min) was subsequently calculated ($f = 60/T_T$). The peak amplitude of the integrated phrenic nerve activity was adjusted in all experiments at similar levels and measured in arbitrary units (AU, cm) on original recordings. The phrenic minute output (neural minute ventilation) was calculated as the product of phrenic tidal activity and respiratory frequency. The slope of the straight line drawn from the onset to 90 % of the maximum level of the phrenic ramp was considered a reliable estimate of the inspiratory rate of rise (e.g. Bongianni et al., 2002, 2008, 2010; Mutolo et al., 2002, 2005; Iovino et al., 2019). Respiratory variables were measured for an average of ten consecutive breaths in the period immediately preceding each trial and at selected times during DAMGO-induced effects (see Results). In the same periods, systolic and diastolic blood pressure were measured at 2-s intervals. Mean arterial pressure was calculated as the diastolic pressure plus one-third of the pulse pressure. Average values for each considered time period were taken along with their coefficient of variation (CV, %) for the purpose of statistical analysis (GraphPad Prism 7, GraphPad Software, Inc., La Jolla, CA, USA). To investigate the excitatory effects of DLH microinjections, average values of ten consecutive breaths were considered before and 30 s after drug administration. In each preparation, we considered respiratory activity fully recovered when respiratory frequency and peak phrenic amplitude were within ± 3% of control values. DAMGO-induced changes in the considered variables were evaluated by means of one-way repeated-measures ANOVA followed by Bonferroni's multiple comparisons tests. DLH effects were analysed by Student's paired *t*-tests. All values are presented as means ± SEM; $P < 0.05$ was considered as significant.

3. Results

3.1. Activation of μ-opioid receptors within the preBötC

Group data of the effects induced by bilateral microinjections of 0.1 and 0.5 mM DAMGO into the preBötC at selected times after the completion of the injections are presented in Figs. 1A and 4 . Bilateral microinjections of 0.1 mM DAMGO (3 − 5 pmol; $n = 5$) into this region induced within 5 min slight, but consistent increases in respiratory frequency. T_T decreased from 1.33 ± 0.05 to 1.1 ± 0.06 s ($P < 0.01$) because of decreases in T_I (from 0.48 ± 0.01 to 0.43 ± 0.01 s; $P < 0.05$) and T_E (from 0.84 ± 0.05 to 0.64 ± 0.05 s; $P < 0.05$). These effects were associated with reductions in peak phrenic amplitude ($P < 0.01$) and the presence of low levels of tonic activity. Slight, not significant decreases in both inspiratory rate of rise and phrenic minute output were present. Peak phrenic amplitude progressively decreased and an irregular pattern of breathing, characterized by phrenic bursts of different amplitudes superimposed on a low level of tonic activity, developed within 10 min (see Fig. 1B). The coefficient of variation of peak phrenic amplitude and time components of the breathing pattern markedly increased (see Fig. 4). The recovery of control respiratory activity occurred progressively and was complete within 60 min.

Bilateral microinjections of 0.5 mM DAMGO (15 − 25 pmol) in the same five preparations caused within 5min significant increases in respiratory frequency. T_T changed from 1.3 ± 0.06 to 0.96 ± 0.05 s ($P < 0.001$) due to decreases in both T_I (from 0.46 ± 0.01 to 0.35 ± 0.01 s; $P < 0.001$) and T_E (from 0.84 ± 0.05 to 0.61 ± 0.05 s; $P < 0.01$). These changes were associated with reductions in peak phrenic amplitude ($P < 0.05$) and increments in inspiratory rate of rise ($P < 0.05$), but not in phrenic minute output. An irregular pattern of breathing consisting of fluctuations in peak phrenic amplitude, associated with a low level of tonic activity ensued within 10 min (Fig. 1C). The coefficient of variation of both time and intensity components of the breathing pattern displayed significant increases (Fig. 4). Apneic

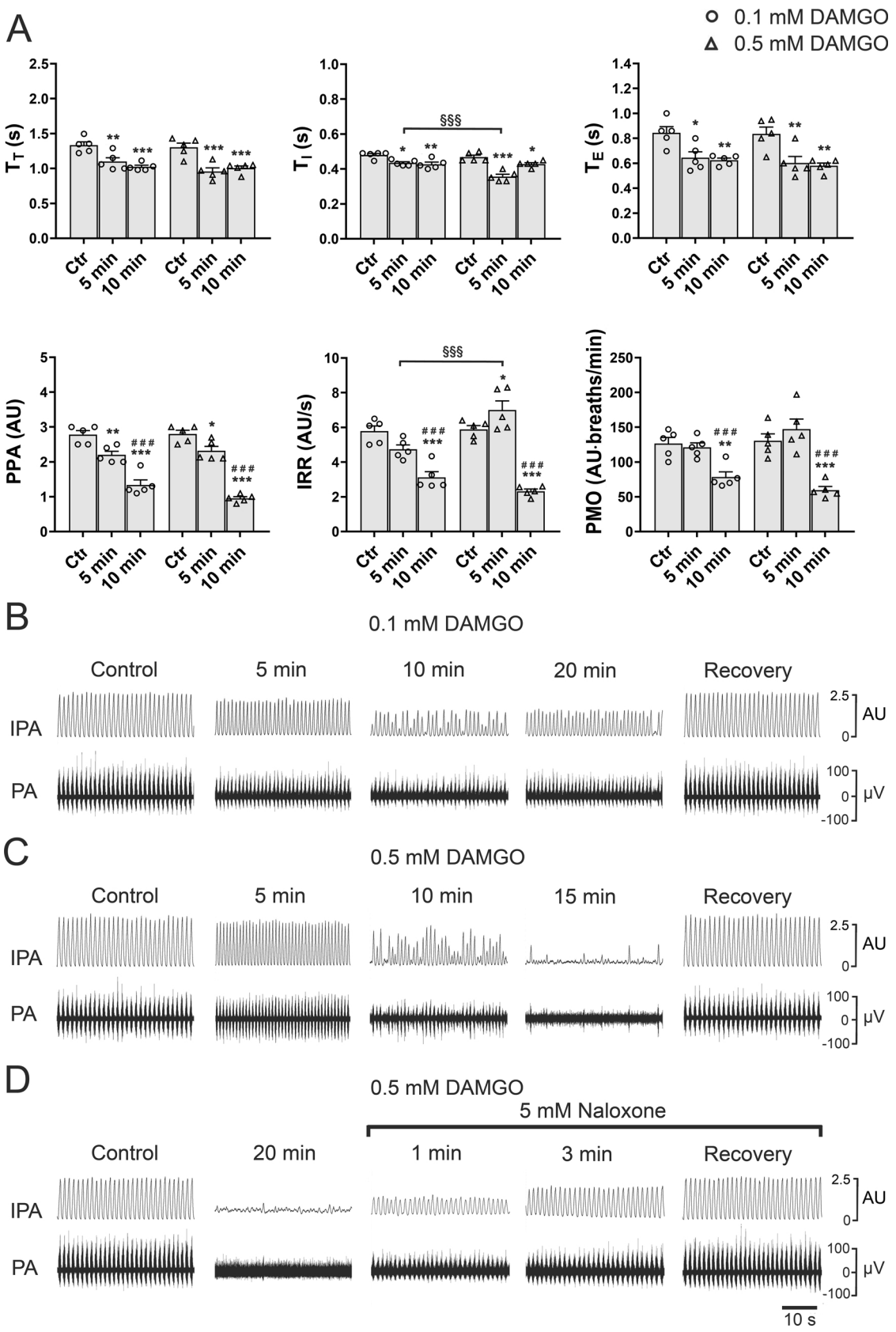

(caption on next page)

effects, characterized by occasional, very weak (ineffective) phrenic bursts superimposed on a higher level of tonic activity, developed within 15 min and lasted for about 25 min (Fig. 1C). In three preparations, respiratory activity recovered within 120 min. In two preparations, the recovery was obtained within 5 min by means of bilateral microinjections of 5 mM naloxone (150 − 250 pmol) into the

Fig. 1. Microinjections of the μ-opioid receptor agonist DAMGO into the preBötC. A: changes in respiratory variables after bilateral microinjections of 0.1 mM (○) and 0.5 mM (△) DAMGO into the preBötC at selected times after the completion of the injections. Abbreviations: T_T, total duration of the respiratory cycle; T_I, inspiratory time; T_E, expiratory time; PPA, peak phrenic amplitude; IRR, inspiratory rate of rise; PMO, phrenic minute output. Individual data points along with means ± SEM are reported. * $P < 0.05$, ** $P < 0.01$, *** $P < 0.001$, compared with control (Ctr); $^{\#\#\#}P < 0.001$, compared with 5 min; $^{\S\S\S}P < 0.001$, compared with 0.1 mM DAMGO. Original recordings showing examples of respiratory responses to bilateral microinjections of 0.1 mM (**B**) and 0.5 mM (**C**) DAMGO at different times after the completion of the injections. A complete recovery occurred within 60 and 120 min, respectively. At the lower DAMGO concentration a partial recovery was already appreciable at 20 min (data at that time not included in the statistical analysis). **D**: an example of reversion of the apneic effects observed about 20 min after 0.5 mM DAMGO by bilateral microinjections of 5 mM naloxone into the same sites. Recovery about 5 min after naloxone. PA, raw phrenic nerve activity; IPA, integrated phrenic nerve activity; AU, arbitrary units (cm).

same sites (Fig. 1D).

3.2. Activation of μ-opioid receptors within the BötC

Group data of the effects induced by bilateral microinjections of 0.1 and 0.5 mM DAMGO into the BötC at selected times after the completion of the injections are shown in Figs. 2A and 4 . Bilateral microinjections of DAMGO into the BötC ($n = 5$) at 0.1 mM caused within 5 min small, but consistent decreases in peak phrenic amplitude ($P < 0.01$) without significant changes in the total duration of the respiratory cycle as well as in the inspiratory rate of rise and phrenic minute output. Peak phrenic activity displayed progressive decreases and within 10 min the pattern of breathing became slightly irregular owing to sparse reductions in peak phrenic amplitude and the development of tonic activity (Fig. 2B). The coefficient of variation of T_T, T_I, T_E and peak phrenic amplitude showed significant increases (Fig. 4). The recovery occurred within 60 min.

Bilateral microinjections of 0.5 mM DAMGO in the same five animals produced within 5 min higher levels of tonic activity and marked decreases in peak phrenic amplitude ($P < 0.001$) without consistent changes in respiratory timing. Both inspiratory rate of rise ($P < 0.01$) and phrenic minute output ($P < 0.001$) decreased. Peak phrenic activity progressively decreased on a background of tonic activity displaying a slight irregular breathing pattern similar to that observed with 0.1 mM DAMGO (not shown). Apnea, characterized by relatively intense tonic phrenic activity, ensued within 25 min (see Fig. 2C). The apneic period was long-lasting (20 − 30 min). A complete recovery was observed within 120 min (3 animals). In two animals, the recovery was achieved within 5 min after bilateral microinjections of 5 mM naloxone performed during the apneic period (not shown).

3.3. Activation of μ-opioid receptors within the iVRG

Group data of the effects induced by bilateral microinjections of 0.1 and 0.5 mM DAMGO into the iVRG at selected times after the completion of the injections are illustrated in Figs. 3A and 4 . Bilateral microinjections of 0.1 mM DAMGO ($n = 5$) into the iVRG induced progressive decreases in peak amplitude and frequency of phrenic bursts. The effects were small and inconsistent after 5 min and reached their maximum about 15 min following the completion of the injections. Peak amplitude of phrenic activity decreased ($P < 0.001$) in association with moderate reductions in respiratory frequency. T_T increased from 1.29 ± 0.03 to 1.73 ± 0.06 ($P < 0.001$) due to increases in both T_I (from 0.5 ± 0.01 to 0.73 ± 0.04 s; $P < 0.001$) and T_E (from 0.78 ± 0.02 to 1.0 ± 0.06 s; $P < 0.01$). Both inspiratory rate of rise ($P < 0.001$) and phrenic minute output ($P < 0.001$) decreased. A complete recovery was observed within 60 min (see also Fig. 3B).

Bilateral microinjections of 0.5 mM DAMGO (same preparations) induced within 5 min significant decreases in peak amplitude ($P < 0.001$) and frequency of phrenic nerve activity. T_T varied from 1.3 ± 0.02 to 1.57 ± 0.02 s ($P < 0.01$) due to increases in both T_I (from 0.5 ± 0.01 to 0.55 ± 0.02 s; $P < 0.05$) and T_E (from 0.83 ± 0.02 to 1.03 ± 0.03 s; $P < 0.01$). These respiratory changes implied decreases in inspiratory rate of rise ($P < 0.001$) and phrenic minute output ($P < 0.001$). The variability of the breathing pattern slightly increased (see Fig. 4). These depressing effects progressively augmented and apnea ensued within 20 min and lasted for about 30 min (Fig. 3C). Rhythmic activity gradually reached the complete recovery within 120 min (3 animals). In two preparations, DAMGO effects were completely reversed within 5 min by bilateral microinjections of 5 mM naloxone (not shown).

3.4. Controls

As in our previous studies on rabbits (e.g. Bongianni et al., 2002, 2008, 2010; Mutolo et al., 2002, 2005; Iovino et al., 2019), injection sites were determined according to stereotaxic coordinates and extracellular neuronal recordings characteristic of each region. Examples of neuronal discharges recorded in each of the three investigated regions are shown in Fig. 5A. The location of the preBötC was ascertained by the presence of excitatory respiratory responses to microinjections of 20 mM DLH. Group data and an example of these excitatory effects are presented in Fig. 5B and C. The location of this region was confirmed by the presence of green fluorescent latex microspheres (Fig. 6). Control microinjections of the vehicle solution in the three investigated regions failed to produce any appreciable effects. All DAMGO-induced respiratory responses occurred without any significant concomitant changes in mean arterial blood pressure that ranged between 90 and 105 mmHg in the different preparations.

4. Discussion

This study provides evidence that not only the preBötC, but also the neighbouring BötC and iVRG contribute to the MOR-induced respiratory depression in the adult anesthetized rabbits. Dose-dependent effects on respiratory activity were induced by MOR-activation in all the investigated regions. At the lower concentration, DAMGO provoked progressive decreases in peak phrenic amplitude that were accompanied by increases (preBötC), no changes (BötC) or decreases (iVRG) in respiratory frequency. These responses occurred either without any concomitant alterations or in association with the appearance of tonic activity and very irregular (preBötC) or slightly irregular (BötC) patterns of breathing. At the higher concentration, DAMGO induced more intense respiratory effects and as final event apneic responses characterized in the preBötC and the BötC by the presence of tonic phrenic nerve activity. The responses to MOR activation by the lower agonist concentration show that especially the preBötC and, to a minor extent, the BötC have a role in the disruption of respiratory rhythmicity. The specificity of DAMGO-induced responses is corroborated by the counteracting action of naloxone and the ineffectiveness of control microinjections. In addition, since respiratory responses were not accompanied by appreciable changes in arterial blood pressure, any role of baroreceptor reflex in their genesis can be ruled out (Daly, 1986). The possible presence of a limited drug diffusion from the injected area to the neighbouring regions cannot be completely ruled out. However, we are confident that the observed DAMGO-induced effects are characteristic of each investigated region since our procedure to reach microinjection target sites derives from results of previous studies in which respiratory effects of different drugs microinjected into the same medullary regions were investigated, and the histological control of injection sites as well as of the spread of the injectate was performed (see Methods). Furthermore, the time course of the development of

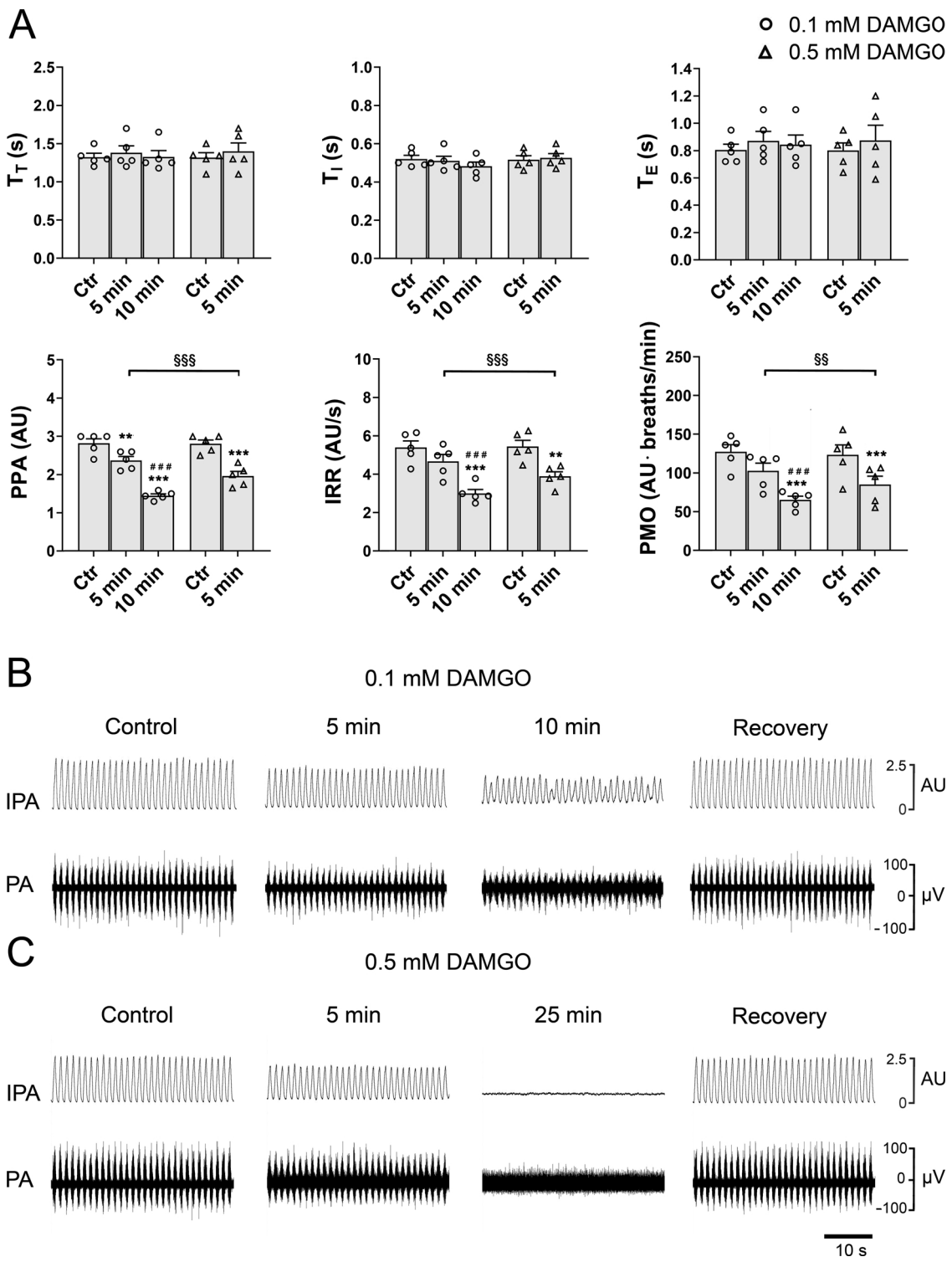

Fig. 2. Microinjections of the μ-opioid receptor agonist DAMGO into the BötC. A: changes in respiratory variables after bilateral microinjections of 0.1 mM (○) and 0.5 mM (△) DAMGO into the BötC at selected times after the completion of the injections. Individual data points along with means ± SEM are reported. ** $P < 0.01$, *** $P < 0.001$, compared with control (Ctr); ### $P < 0.001$, compared with 5 min; §§ $P < 0.01$, §§§ $P < 0.001$, compared with 0.1 mM DAMGO. Original recordings showing examples of respiratory responses to bilateral microinjections of 0.1 mM (**B**) and 0.5 mM (**C**) DAMGO at different times after the completion of the injections. Recovery after 60 and 120 min, respectively. For abbreviations see Fig. 1.

DAMGO-induced changes and the final effects display clear differences in the three regions (see Results). In agreement with previous findings (Prkic et al., 2012; Levitt et al., 2015; Stucke et al., 2015; Varga et al., 2020), present results indicate that different regions of the brainstem respiratory network may be involved in the genesis of opioid-induced respiratory disorders. They are also consistent with the view that respiratory pattern formation engages distributed neuronal populations within the different brainstem respiratory compartments (see e.g. Von Euler, 1997; Mutolo et al., 2002; Smith et al., 2007; Dhingra et al., 2019, 2020 also for further Refs.).

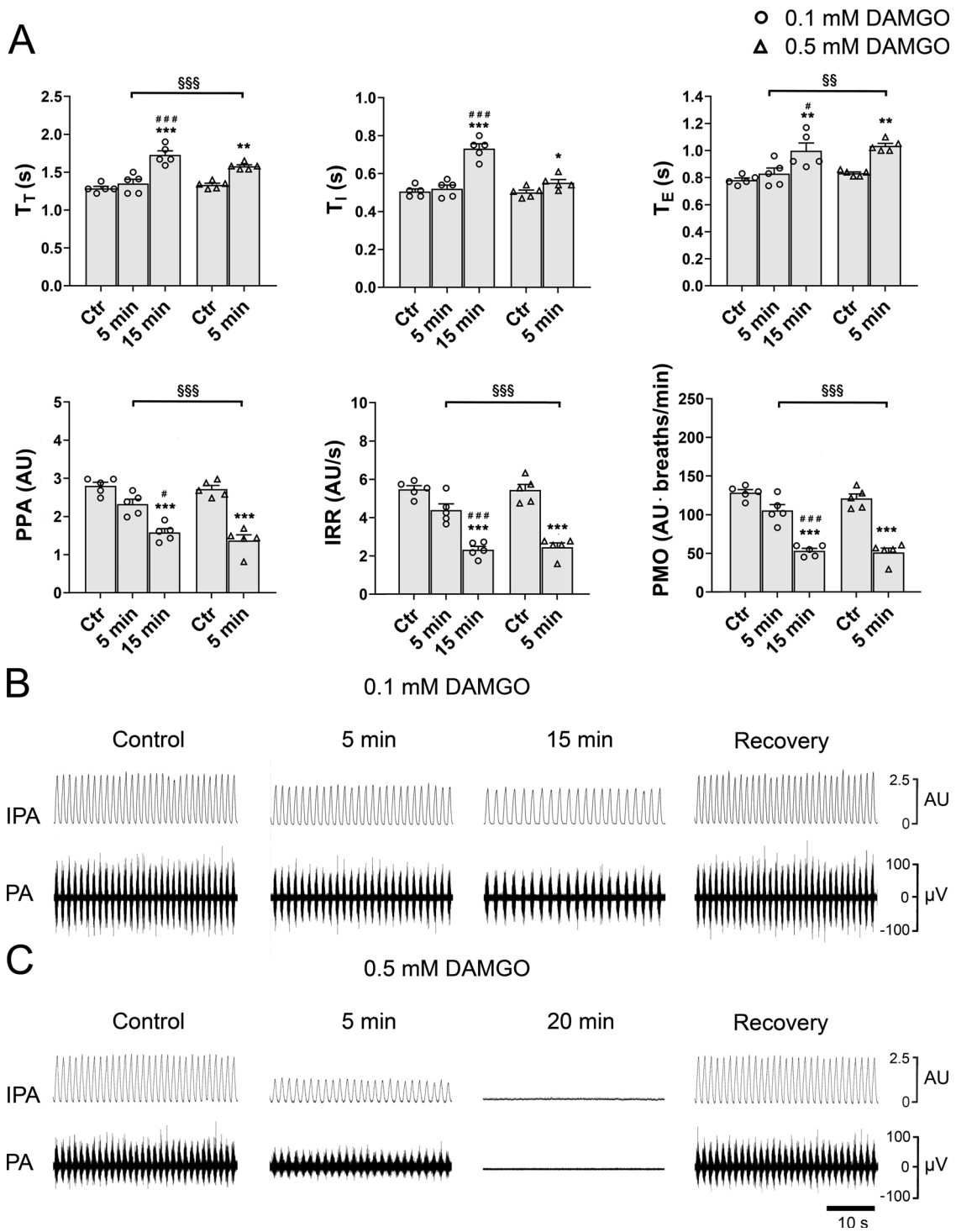

Fig. 3. Microinjections of the μ-opioid receptor agonist DAMGO into the iVRG. A: changes in respiratory variables after bilateral microinjections of 0.1 mM (○) and 0.5 mM (△) DAMGO into the iVRG at selected times after the completion of the injections. Individual data points along with means ± SEM are reported. * $P < 0.05$, ** $P < 0.01$, *** $P < 0.001$, compared with control (Ctr); $^{\#}$ $P < 0.05$, $^{\#\#\#}$ $P < 0.001$, compared with 5 min; §§ $P < 0.01$, §§§ $P < 0.001$, compared with 0.1 mM DAMGO. Original recordings showing examples of respiratory responses to bilateral microinjections of 0.1 mM (**B**) and 0.5 mM (**C**) DAMGO at different times after the completion of the injections. Recovery after 60 and 120 min, respectively. For abbreviations see Fig. 1.

4.1. DAMGO-induced respiratory responses in the preBötC

Our results are consistent with previous findings suggesting an important role of the preBötC in MOR-induced respiratory depression. It has been shown that the preBötC contributes to respiratory depression in medullary slices of neonatal rodents (Gray et al., 1999; Sun et al., 2019) or in anesthetized or conscious adult rats (Montandon et al., 2011, 2016) as well as in anesthetized, paralyzed and artificially ventilated adult rats (Qi et al., 2017). However, doubts have been casted on the role of the preBötC. It has been found that MOR activation within this region causes consistent increases in respiratory frequency accompanied by inconsistent or relatively small decreases in peak phrenic activity in adult anesthetized, paralyzed, vagotomized and artificially ventilated rats (Lonergan et al., 2003) and in decerebrated, paralyzed,

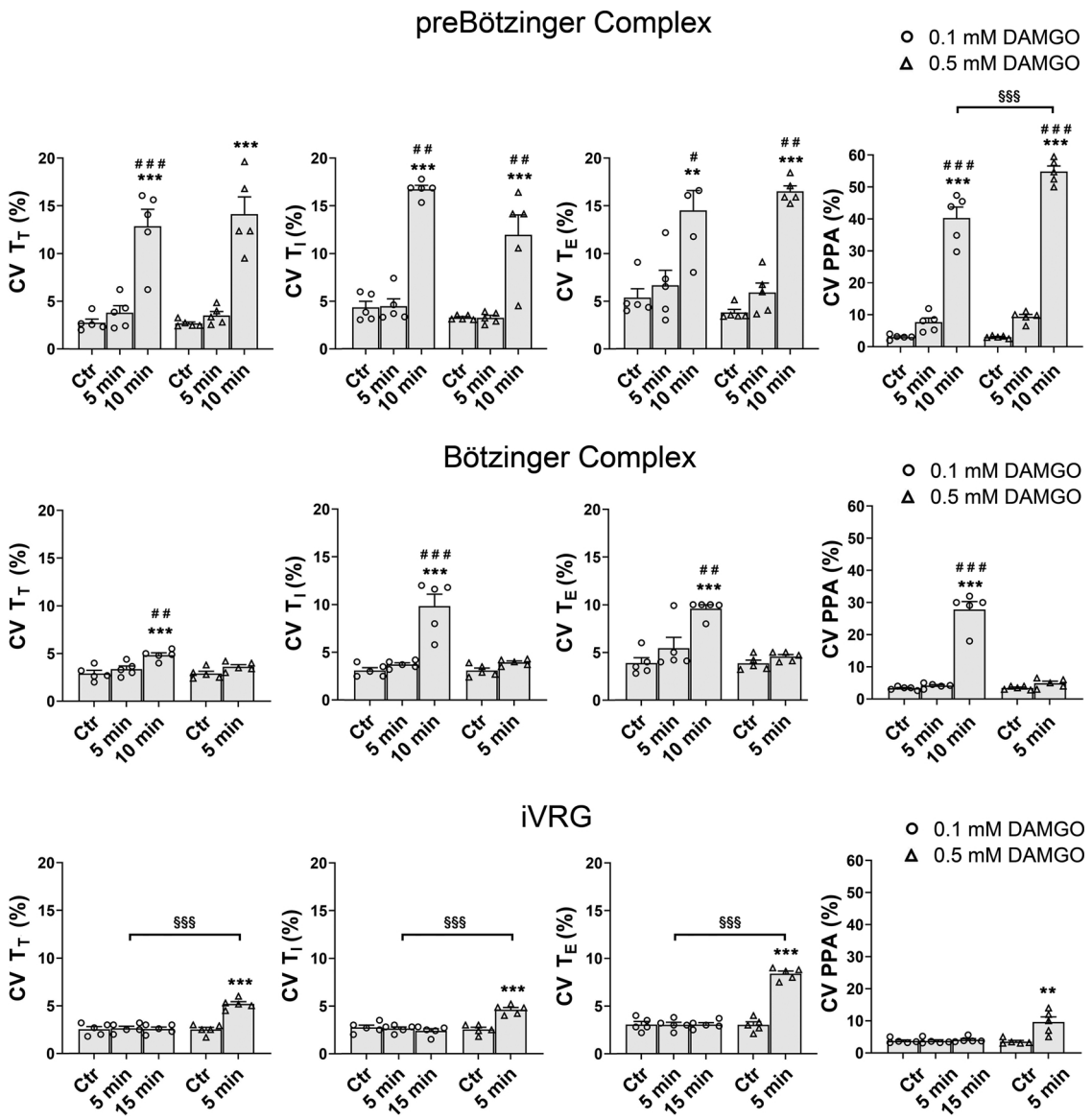

Fig. 4. DAMGO-induced changes in the coefficient of variation of the intensity and time components of the breathing pattern. Changes in the coefficient of variation (CV, %) of some respiratory variables after bilateral microinjections of 0.1 mM (○) and 0.5 mM (△) DAMGO into the three investigated medullary regions at selected times after the completion of the injections. Individual data points along with means ± SEM are reported. ** $P < 0.01$, *** $P < 0.001$, compared with control (Ctr); ## $P < 0.01$, ### $P < 0.001$, compared with 5 min; §§§ $P < 0.001$, compared with 0.1 mM DAMGO. Note that CV increases were particularly pronounced after DAMGO microinjections into the preBötC. For abbreviations see Fig. 1.

and artificially ventilated dogs (Mustapic et al., 2010). In addition, DAMGO microinjections into the preBötC of the awake adult goat had no effects on eupneic breathing (Krause et al., 2009). Stucke et al. (2015) studied the effects of DAMGO microinjections into the preBötC as well as those of the systemic administration of the opioid agonist remifentanil in decerebrated, paralyzed, and artificially ventilated young and adult rabbits. Both local DAMGO and systemic remifentanil caused both respiratory depression and changes in respiratory timing. Naloxone microinjections into the preBötC completely reversed the effects of local DAMGO administration. Interestingly, remifentanil effects were completely antagonized by intravenous, but not by local naloxone, thus leading to the conclusion that systemic opioids also affect respiratory components outside the preBötC. Recently, both the preBötC and the pontine parabrachial and KF nuclei have been shown to play a role in the opioid-induced respiratory depression (Levitt et al., 2015; Miller et al., 2017; Varga et al., 2020). In particular, Varga et al. (2020) using a genetic approach to conditionally delete MORs within the KF nucleus or the preBötC in awake adult mice demonstrated that both regions have a role, with a major impact of the KF nucleus. They concluded that opioids affect distributed areas of the respiratory network and that opioid-induced respiratory disturbances cannot be ascribed to a single region. These results are not surprising owing to the dense reciprocal connections between the KF nucleus and the preBötC (Ezure and Tanaka, 2006; Tan et al., 2010; Song et al., 2012; Yokota et al., 2015; Geerling et al., 2017; Yang and Feldman, 2018).

The cause of the conflicting results is obscure. Differences in the animal species, the type of preparation and the experimental procedures employed could be involved. In addition, all methodological approaches have their own limitations that may affect the reliability of obtained results. The state of consciousness may also strongly modify the role of the preBötC (see e.g. McKay et al., 2005; Montandon and Horner, 2013, 2014). In agreement with Varga et al. (2020), in most studies, with the exception of that of Montandon et al. (2016), it is unknown if the effects of systemic opioids are due to locally expressed somatodendritic or presynaptic MORs or to MORs located on terminals in projection regions. Furthermore, during systemic opioid

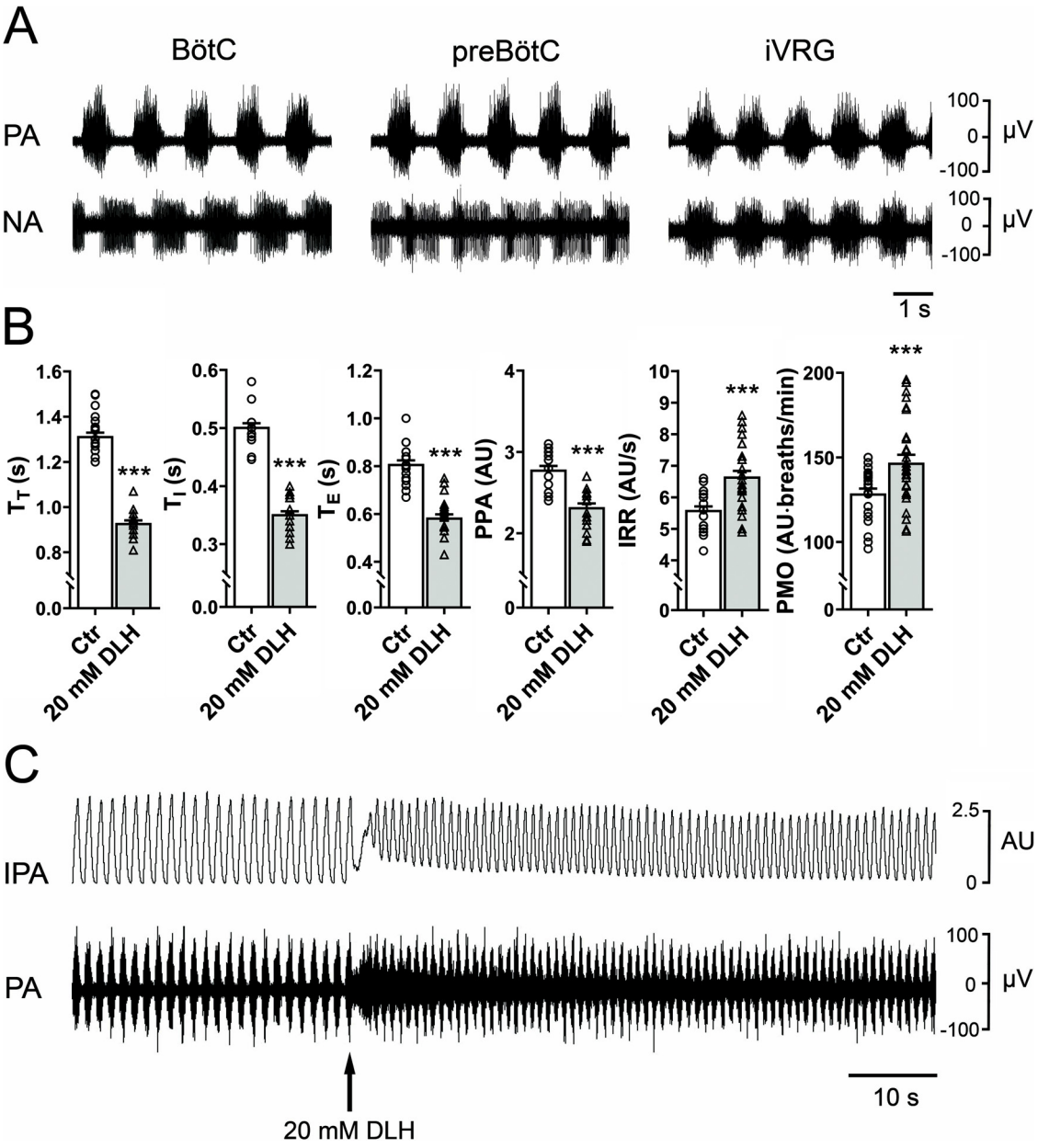

Fig. 5. Localization of injection sites. A: examples of extracellular recordings of the pattern of discharge of neurons encountered in each of the three investigated regions. NA, neuronal activity. **B**: changes induced by 20mM D, L-homocisteic acid (DLH) microinjections into the preBötC in some variables of the pattern of breathing (30 trials). Individual data points along with means ± SEM are reported. *** $P < 0.001$, compared with control (Ctr). **C**: characteristic excitatory response to a unilateral microinjection of 20 mM DLH into the preBötC. For abbreviations see Fig. 1.

administration a locally applied antagonist will leave still inhibited terminals in projection areas. In addition, opioids probably act not only on the already well known components of the brainstem respiratory network, but also on other brain areas, for instance those involved in nociception, that may in turn affect respiration (e.g. Jiang et al., 2004).

It seems worth noting that an irregular (ataxic) breathing pattern was already observed in response to microinjections of DAMGO at the lower concentration (see Figs. 1B and 4). This is consistent with the notion that irregular breathing is an important component of MOR-induced respiratory depression (Bouillon et al., 2003; Pattinson, 2008) and that a disrupted pattern of breathing could be life-threatening likewise complete apnea (see also Varga et al., 2020). Ataxic breathing was also induced by activation of MORs located in the KF nucleus that, as already mentioned, has dense reciprocal connections with the preBötC. DAMGO-induced responses in the preBötC characterized by increases in respiratory frequency associated with decreases in peak phrenic amplitude and the development of tonic phrenic activity are reminiscent of those obtained with microinjections of the neurotoxin kainic acid (Mutolo et al., 2002), the selective NMDA receptor antagonist D-AP5 and the broad-spectrum EAA receptor antagonist kynurenic acid (Mutolo et al., 2005). We did not observe "quantal slowing", i.e. increased expiratory periods resulting from skipped inspiration (Mellen et al., 2003; Pattinson, 2008; Lal et al., 2011; Baesens and Mackay, 2013), probably due to differences in the preparation and the drug employed. Accordingly, Mellen et al. (2003) observed quantal slowing in anesthetized, vagotomized, juvenile rats in response to fentanyl.

At present, an exhaustive explanation of all DAMGO respiratory effects is not available. However, an important role of the removal of inhibitory mechanisms in the generation of altered breathing patterns has been suggested in previous reports (see e.g. Pierrefiche et al., 1998; Mutolo et al., 2002, 2005; Bongianni et al., 2010; Varga et al., 2020). In

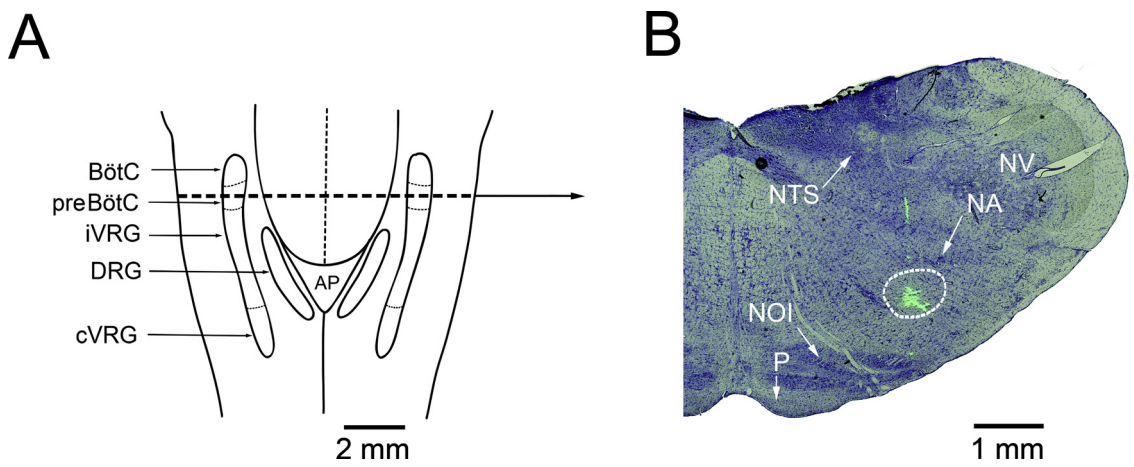

Fig. 6. Histological localization of the preBötC. A: diagrammatic representation of the dorsal view of the rabbit medulla oblongata showing some components of the respiratory network. AP, area postrema; BötC, Bötzinger complex; cVRG, caudal ventral respiratory group; DRG, dorsal respiratory group; iVRG, inspiratory ventral respiratory group; preBötC, preBötzinger complex. **B**: photomicrograph of a coronal section of the medulla oblongata at the level indicated by the dashed line (about 2.5 mm rostral to the obex) showing an example of the location of fluorescent microspheres microinjected into the preBötC. The histological section is counterstained with Cresyl violet. Light-field and fluorescent photomicrographs have been superimposed. NA, nucleus ambiguus; NOI, nucleus olivaris inferior; NTS, nucleus tractus solitarii; NV, nucleus tractus spinalis nervi trigemini; P, tractus pyramidalis.

addition, we can propose an involvement of pontine influences on both the preBötC and the BötC (see below) in the development of apnea associated with intense tonic phrenic nerve activity that reminds apneusis (St John, 1998). Pontine influences on respiration imply both excitatory and inhibitory pathways and are mediated, at least in part, by parabrachial and KF nuclei (Von Euler, 1986; Chamberlin and Saper, 1994; Bianchi et al., 1995; Mutolo et al., 1998; Pierrefiche et al., 1998; see also Dutschmann and Herbert, 2006; Dutschmann and Dick, 2012; Jones et al., 2016).

4.2. DAMGO-induced respiratory responses in the BötC and the iVRG

DAMGO-induced irregular patterns of breathing associated with tonic phrenic activity as well as the appearance of tonic apnea within the BötC display similarities with the effects observed following MOR activation in the preBötC. Since the BötC is one of the main source of inhibition in the respiratory network (see e.g. Lipski and Merrill, 1980; Fedorko and Merrill, 1984; Von Euler, 1986; Jiang and Shen, 1991; Bianchi et al., 1995; Bongianni et al., 1997; Iscoe, 1998; Mutolo et al., 2002), these results could be ascribed to a DAMGO-induced silencing of BötC neurons and are consistent with the interpretation that a lack of inhibitory mechanisms underlies respiratory responses elicited in the BötC and, possibly, also those observed in the preBötC, if the activation of MORs on terminals of BötC projections is hypothesized. Unexpectedly, in the first period after the microinjections into the BötC DAMGO did not produce consistent changes in respiratory frequency, but only decreases in peak phrenic amplitude. This outcome is obscure. However, it should be remembered that the population of BötC is far from being homogenous since it contains both excitatory and inhibitory neurons with different patterns of discharge (e.g. Bongianni et al., 1997, 2010; for review see Iscoe, 1998).

Decreases in peak phrenic amplitude and, in particular, apnea without concomitant tonic activity following DAMGO microinjections into the iVRG are not surprising since they can be ascribed to an inhibitory action on inspiratory bulbospinal neurons that are largely concentrated in this region (e.g. Von Euler, 1986; Bianchi et al., 1995). Present findings are consistent with previous results obtained with microinjections of EAA receptor antagonists into this region (Bongianni et al., 2002). It seems relevant to mention that the respiratory depression due to reductions in respiratory frequency is a common feature of systemic opioid administration (see e.g. Pattinson, 2008; Dahan et al., 2010; Prkic et al., 2012). Interestingly, DAMGO-induced reductions in respiratory frequency strongly suggest that this region does not merely represent an inspiratory output system, but is also involved in the timing control of the respiratory pattern generator via its connections with other respiration-related areas (Ellenberger and Feldman, 1990; Jones et al., 2016).

4.3. Concluding remarks

Present results provide further insights into the role of MORs in the genesis of respiratory depression induced by systemically administered opioids. They confirm that the preBötC may play a prominent role, but also indicate that the action of opioids within other areas of the respiratory network should be considered. The results also suggest that various areas of the respiratory network differentially contribute to the opioid-induced respiratory disturbances for instance causing reductions in peak amplitude and frequency of inspiratory activity as well as irregular patterns of breathing with a concomitant development of tonic activity and apneustic effects or apneas. Finally, it cannot be ruled out that also brain areas outside the brainstem respiratory network may contribute to the depressing effects.

Funding

This study was supported by grants from the University of Florence and from theEnte Cassa di Risparmio Firenze, Italy. EC is supported by a postdoctoral fellowship from the University of Florence.

Author contributions

E.C., F.B., T.P. and D.M. conception and design of research; E.C., F.B. and D.M. performed experiments; E.C. and D.M. analyzed data; E.C., F.B., T.P. and D.M. interpreted results of experiments; E.C. prepared figures; E.C., T.P. and D.M. drafted manuscript; E.C., F.B., T.P. and D.M. edited and revised manuscript; E.C., F.B., T.P. and D.M. approved final version of the manuscript.

Declaration of Competing Interest

The authors declare that they have no competing interest.

References

Anderson, T.M., Ramirez, J.M., 2017. Respiratory rhythm generation: triple oscillator hypothesis. F1000Res. 6, 139.

Anderson, T.M., Garcia III, A.J., Baertsch, N.A., Pollak, J., Bloom, J.C., Wei, A.D., Rai, K.G., Ramirez, J.M., 2016. A novel excitatory network for the control of breathing. Nature 536, 76–80.

Baesens, C., Mackay, R., 2013. Analysis of a scenario for chaotic quantal slowing down of inspiration. J. Math. Neurosci. 3, 18.

Bianchi, A.L., Denavit-Saubie, M., Champagnat, J., 1995. Central control of breathing in mammals: neuronal circuitry, membrane properties, and neurotransmitters. Physiol. Rev. 75, 1–45.

Bongianni, F., Mutolo, D., Pantaleo, T., 1997. Depressant effects on inspiratory and expiratory activity produced by chemical activation of Bötzinger complex neurons in the rabbit. Brain Res. 749, 1–9.

Bongianni, F., Mutolo, D., Carfi, M., Pantaleo, T., 2002. Respiratory responses to ionotropic glutamate receptor antagonists in the ventral respiratory group of the rabbit. Pflügers Arch. 444, 602–609.

Bongianni, F., Mutolo, D., Cinelli, E., Pantaleo, T., 2008. Neurokinin receptor modulation of respiratory activity in the rabbit. Eur. J. Neurosci. 27, 3233–3243.

Bongianni, F., Mutolo, D., Cinelli, E., Pantaleo, T., 2010. Respiratory responses induced by blockades of GABA and glycine receptors within the Bötzinger complex and the pre-Bötzinger complex of the rabbit. Brain Res. 1344, 134–147.

Bouillon, T., Bruhn, J., Roepcke, H., Hoeft, A., 2003. Opioid-induced respiratory depression is associated with increased tidal volume variability. Eur. J. Anaesthesiol. 20, 127–133.

Chamberlin, N.L., Saper, C.B., 1994. Topographic organization of respiratory responses to glutamate microstimulation of the parabrachial nucleus in the rat. J. Neurosci. 14, 6500–6510.

Connelly, C.A., Dobbins, E.G., Feldman, J.L., 1992. Pre-Bötzinger complex in cats: respiratory neuronal discharge patterns. Brain Res. 590, 337–340.

Dahan, A., Aarts, L., Smith, T.W., 2010. Incidence, reversal, and prevention of opioid-induced respiratory depression. Anesthesiology 112, 226–238.

Daly, M.B.D., 1986. Interactions between respiration and circulation. In: Cherniack, N.S., Widdicombe, J.G. (Eds.), Handbook of Physiology. The Respiratory System. Control of Breathing. American Physiological Society, Bethesda, MD, pp. 529–594.

Dang, V.C., Christie, M.J., 2012. Mechanisms of rapid opioid receptor desensitization, resensitization and tolerance in brain neurons. Br. J. Pharmacol. 165, 1704–1716.

Del Negro, C.A., Funk, G.D., Feldman, J.L., 2018. Breathing matters. Nat. Rev. Neurosci. 19, 351–367.

Dhingra, R.R., Furuya, W.I., Bautista, T.G., Dick, T.E., Galan, R.F., Dutschmann, M., 2019. Increasing local excitability of brainstem respiratory nuclei reveals a distributed network underlying respiratory motor pattern formation. Front. Physiol. 10, 887.

Dhingra, R.R., Dick, T.E., Furuya, W.I., Galan, R.F., Dutschmann, M., 2020. Volumetric mapping of the functional neuroanatomy of the respiratory network in the perfused brainstem preparation of rats. J. Physiol. 598, 2061–2079.

Dutschmann, M., Dick, T.E., 2012. Pontine mechanisms of respiratory control. Compr. Physiol. 2, 2443–2469.

Dutschmann, M., Herbert, H., 2006. The Kolliker-Fuse nucleus gates the postinspiratory phase of the respiratory cycle to control inspiratory off-switch and upper airway resistance in rat. Eur. J. Neurosci. 24, 1071–1084.

Ellenberger, H.H., Feldman, J.L., 1990. Brainstem connections of the rostral ventral respiratory group of the rat. Brain Res. 513, 35–42.

Ezure, K., Tanaka, I., 2006. Distribution and medullary projection of respiratory neurons in the dorsolateral pons of the rat. Neuroscience 141, 1011–1023.

Fedorko, L., Merrill, E.G., 1984. Axonal projections from the rostral expiratory neurones of the Botzinger complex to medulla and spinal cord in the cat. J. Physiol. 350, 487–496.

Feldman, J.L., Del Negro, C.A., 2006. Looking for inspiration: new perspectives on respiratory rhythm. Nat. Rev. Neurosci. 7, 232–242.

Feldman, J.L., Mitchell, G.S., Nattie, E.E., 2003. Breathing: Rhythmicity, Plasticity, Chemosensitivity. Annu. Rev. Neurosci. 26, 239–266.

Feldman, J.L., Del Negro, C.A., Gray, P.A., 2013. Understanding the rhythm of breathing: so near, yet so far. Annu. Rev. Physiol. 75, 423–452.

Geerling, J.C., Yokota, S., Rukhadze, I., Roe, D., Chamberlin, N.L., 2017. Kölliker-Fuse GABAergic and glutamatergic neurons project to distinct targets. J. Comp. Neurol. 525, 1844–1860.

Gray, P.A., Rekling, J.C., Bocchiaro, C.M., Feldman, J.L., 1999. Modulation of respiratory frequency by peptidergic input to rhythmogenic neurons in the preBötzinger complex. Science 286, 1566–1568.

Gray, P.A., Janczewski, W.A., Mellen, N., McCrimmon, D.R., Feldman, J.L., 2001. Normal breathing requires preBötzinger complex neurokinin-1 receptor- expressing neurons. Nat. Neurosci. 4, 927–930.

Iovino, L., Mutolo, D., Cinelli, E., Contini, M., Pantaleo, T., Bongianni, F., 2019. Breathing stimulation mediated by 5-HT1A and 5-HT3 receptors within the preBötzinger complex of the adult rabbit. Brain Res. 1704, 26–39.

Iscoe, S., 1998. Control of abdominal muscles. Prog. Neurobiol. 56, 433–506.

Jiang, C., Shen, E., 1991. Respiratory neurons in the medulla of the rabbit: distribution, discharge patterns and spinal projections. Brain Res. 541, 284–292.

Jiang, M., Alheid, G.F., Calandriello, T., McCrimmon, D.R., 2004. Parabrachial-lateral pontine neurons link nociception and breathing. Respir. Physiol. Neurobiol. 143, 215–233.

Jones, S.E., Stanic, D., Dutschmann, M., 2016. Dorsal and ventral aspects of the most caudal medullary reticular formation have differential roles in modulation and formation of the respiratory motor pattern in rat. Brain Struct. Funct. 221, 4353–4368.

Krause, K.L., Neumueller, S.E., Marshall, B.D., Kiner, T., Bonis, J.M., Pan, L.G., Qian, B., Forster, H.V., 2009. μ-opioid receptor agonist injections into the presumed pre-Bötzinger complex and the surrounding region of awake goats do not alter eupneic breathing. J. Appl. Physiol. 107, 1591–1599.

Krolo, M., Tonkovic-Capin, V., Stucke, A.G., Stuth, E.A., Hopp, F.A., Dean, C., Zuperku, E.J., 2005. Subtype composition and responses of respiratory neurons in the pre-Bötzinger region to pulmonary afferent inputs in dogs. J. Neurophysiol. 93, 2674–2687.

Lal, A., Oku, Y., Hulsmann, S., Okada, Y., Miwakeichi, F., Kawai, S., Tamura, Y., Ishiguro, M., 2011. Dual oscillator model of the respiratory neuronal network generating quantal slowing of respiratory rhythm. J. Comput. Neurosci. 30, 225–240.

Lalley, P.M., 2003. Mu-opioid receptor agonist effects on medullary respiratory neurons in the cat: evidence for involvement in certain types of ventilatory disturbances. Am. J. Physiol. Regul. Integr. Comp. Physiol. 285, R1287–1304.

Levitt, E.S., Abdala, A.P., Paton, J.F., Bissonnette, J.M., Williams, J.T., 2015. Mu opioid receptor activation hyperpolarizes respiratory-controlling Kölliker-Fuse neurons and suppresses post-inspiratory drive. J. Physiol. 593, 4453–4469.

Lipski, J., Merrill, E.G., 1980. Electrophysiological demonstration of the projection from expiratory neurones in rostral medulla to contralateral dorsal respiratory group. Brain Res. 197, 521–524.

Lipski, J., Bellingham, M.C., West, M.J., Pilowsky, P., 1988. Limitations of the technique of pressure microinjection of excitatory amino acids for evoking responses from localized regions of the CNS. J. Neurosci. Methods 26, 169–179.

Lonergan, T., Goodchild, A.K., Christie, M.J., Pilowsky, P.M., 2003. Mu opioid receptors in rat ventral medulla: effects of endomorphin-1 on phrenic nerve activity. Respir. Physiol. Neurobiol. 138, 165–178.

Lumsden, T., 1923. Observations on the respiratory centres in the cat. J. Physiol. 57, 153–160.

Mansour, A., Fox, C.A., Burke, S., Meng, F., Thompson, R.C., Akil, H., Watson, S.J., 1994. Mu, delta, and kappa opioid receptor mRNA expression in the rat CNS: an in situ hybridization study. J. Comp. Neurol. 350, 412–438.

McKay, L.C., Janczewski, W.A., Feldman, J.L., 2005. Sleep-disordered breathing after targeted ablation of preBötzinger complex neurons. Nat. Neurosci. 8, 1142–1144.

Mellen, N.M., Janczewski, W.A., Bocchiaro, C.M., Feldman, J.L., 2003. Opioid-induced quantal slowing reveals dual networks for respiratory rhythm generation. Neuron 37, 821–826.

Miller, J.R., Zuperku, E.J., Stuth, E.A.E., Banerjee, A., Hopp, F.A., Stucke, A.G., 2017. A subregion of the parabrachial nucleus partially mediates respiratory rate depression from intravenous remifentanil in young and adult rabbits. Anesthesiology 127, 502–514.

Monnier, A., Alheid, G.F., McCrimmon, D.R., 2003. Defining ventral medullary respiratory compartments with a glutamate receptor agonist in the rat. J. Physiol. 548, 859–874.

Montandon, G., Horner, R.L., 2013. State-dependent contribution of the hyperpolarization-activated Na+/K+ and persistent Na+ currents to respiratory rhythmogenesis in vivo. J. Neurosci. 33, 8716–8728.

Montandon, G., Horner, R., 2014. CrossTalk proposal: the preBötzinger complex is essential for the respiratory depression following systemic administration of opioid analgesics. J. Physiol. 592, 1159–1162.

Montandon, G., Qin, W., Liu, H., Ren, J., Greer, J.J., Horner, R.L., 2011. PreBötzinger complex neurokinin-1 receptor-expressing neurons mediate opioid-induced respiratory depression. J. Neurosci. 31, 1292–1301.

Montandon, G., Liu, H., Horner, R.L., 2016. Contribution of the respiratory network to rhythm and motor output revealed by modulation of GIRK channels, somatostatin and neurokinin-1 receptors. Sci. Rep. 6, 32707.

Mustapic, S., Radocaj, T., Sanchez, A., Dogas, Z., Stucke, A.G., Hopp, F.A., Stuth, E.A., Zuperku, E.J., 2010. Clinically relevant infusion rates of mu-opioid agonist remifentanil cause bradypnea in decerebrate dogs but not via direct effects in the pre-Bötzinger complex region. J. Neurophysiol. 103, 409–418.

Mutolo, D., Bongianni, F., Carfi, M., Pantaleo, T., 1998. Respiratory responses to chemical stimulation of the parabrachial nuclear complex in the rabbit. Brain Res. 807, 182–186.

Mutolo, D., Bongianni, F., Carfi, M., Pantaleo, T., 2002. Respiratory changes induced by kainic acid lesions in rostral ventral respiratory group of rabbits. Am. J. Physiol. Regul. Integr. Comp. Physiol. 283, R227–R242.

Mutolo, D., Bongianni, F., Nardone, F., Pantaleo, T., 2005. Respiratory responses evoked by blockades of ionotropic glutamate receptors within the Bötzinger complex and the pre-Bötzinger complex of the rabbit. Eur. J. Neurosci. 21, 122–134.

Mutolo, D., Bongianni, F., Cinelli, E., Fontana, G.A., Pantaleo, T., 2008. Modulation of the cough reflex by antitussive agents within the caudal aspect of the nucleus tractus solitarii in the rabbit. Am. J. Physiol. Regul. Integr. Comp. Physiol. 295, R243–R251.

Mutolo, D., Bongianni, F., Cinelli, E., Pantaleo, T., 2010. Depression of cough reflex by microinjections of antitussive agents into caudal ventral respiratory group of the rabbit. J. Appl. Physiol. 109, 1002–1010.

Nicholson, C., 1985. Diffusion from an injected volume of a substance in brain tissue with arbitrary volume fraction and tortuosity. Brain Res. 333, 325–329.

Nicholson, C., Sykova, E., 1998. Extracellular space structure revealed by diffusion analysis. Trends Neurosci. 21, 207–215.

Pantaleo, T., Mutolo, D., Cinelli, E., Bongianni, F., 2011. Respiratory responses to somatostatin microinjections into the Bötzinger complex and the pre-Bötzinger complex of the rabbit. Neurosci. Lett. 498, 26–30.

Pattinson, K.T., 2008. Opioids and the control of respiration. Br. J. Anaesth. 100, 747–758.

Pierrefiche, O., Schwarzacher, S.W., Bischoff, A.M., Richter, D.W., 1998. Blockade of synaptic inhibition within the pre-Bötzinger complex in the cat suppresses respiratory rhythm generation in vivo. J. Physiol. 509, 245–254.

Prkic, I., Mustapic, S., Radocaj, T., Stucke, A.G., Stuth, E.A., Hopp, F.A., Dean, C., Zuperku, E.J., 2012. Pontine mu-opioid receptors mediate bradypnea caused by intravenous remifentanil infusions at clinically relevant concentrations in dogs. J. Neurophysiol. 108, 2430–2441.
Qi, J., Li, H., Zhao, T.B., Lu, Y.C., Zhang, T., Li, J.L., Dong, Y.L., Li, Y.Q., 2017. Inhibitory effect of Endomorphin-2 binding to the mu-opioid receptor in the rat pre-Bötzinger complex on the breathing activity. Mol. Neurobiol. 54, 461–469.
Radocaj, T., Mustapic, S., Prkic, I., Stucke, A.G., Hopp, F.A., Stuth, E.A., Zuperku, E.J., 2015. Activation of 5-HT1A receptors in the preBötzinger region has little impact on the respiratory pattern. Respir. Physiol. Neurobiol. 212–214, 9–19.
Rekling, J.C., Feldman, J.L., 1998. PreBötzinger complex and pacemaker neurons: hypothesized site and kernel for respiratory rhythm generation. Annu. Rev. Physiol. 60, 385–405.
Schwarzacher, S.W., Smith, J.C., Richter, D.W., 1995. Pre-Bötzinger complex in the cat. J. Neurophysiol. 73, 1452–1461.
Shek, J.W., Wen, G.Y., Wisniewski, H.M., 1986. Atlas of the Rabbit Brain and Spinal Cord. Karger, Basel.
Smith, J.C., Ellenberger, H.H., Ballanyi, K., Richter, D.W., Feldman, J.L., 1991. Pre-Bötzinger complex: a brainstem region that may generate respiratory rhythm in mammals. Science 254, 726–729.
Smith, J.C., Abdala, A.P., Koizumi, H., Rybak, I.A., Paton, J.F., 2007. Spatial and functional architecture of the mammalian brain stem respiratory network: a hierarchy of three oscillatory mechanisms. J. Neurophysiol. 98, 3370–3387.
Solomon, I.C., Edelman, N.H., Neubauer, J.A., 1999. Patterns of phrenic motor output evoked by chemical stimulation of neurons located in the pre-Bötzinger complex in vivo. J. Neurophysiol. 81, 1150–1161.
Song, G., Wang, H., Xu, H., Poon, C.S., 2012. Kölliker-Fuse neurons send collateral projections to multiple hypoxia-activated and nonactivated structures in rat brainstem and spinal cord. Brain Struct. Funct. 217, 835–858.
St John, W.M., 1998. Neurogenesis of patterns of automatic ventilatory activity. Prog. Neurobiol. 56, 97–117.
St-John, W.M., Paton, J.F., 2004. Role of pontile mechanisms in the neurogenesis of eupnea. Respir. Physiol. Neurobiol. 143, 321–332.
Stucke, A.G., Miller, J.R., Prkic, I., Zuperku, E.J., Hopp, F.A., Stuth, E.A., 2015. Opioid-induced respiratory depression is only partially mediated by the preBötzinger complex in young and adult rabbits in vivo. Anesthesiology 122, 1288–1298.
Sun, X., Thorn Perez, C., Halemani, D.N., Shao, X.M., Greenwood, M., Heath, S., Feldman, J.L., Kam, K., 2019. Opioids modulate an emergent rhythmogenic process to depress breathing. Elife 8.
Tan, W., Janczewski, W.A., Yang, P., Shao, X.M., Callaway, E.M., Feldman, J.L., 2008. Silencing preBötzinger complex somatostatin-expressing neurons induces persistent apnea in awake rat. Nat. Neurosci. 11, 538–540.
Tan, W., Pagliardini, S., Yang, P., Janczewski, W.A., Feldman, J.L., 2010. Projections of preBötzinger Complex neurons in adult rats. J. Comp. Neurol. 518, 1862–1878.
Toor, R., Sun, Q.J., Kumar, N.N., Le, S., Hildreth, C.M., Phillips, J.K., McMullan, S., 2019. Neurons in the intermediate reticular nucleus coordinate postinspiratory activity, swallowing, and respiratory-sympathetic coupling in the rat. J. Neurosci. 39, 9757–9766.
Varga, A.G., Reid, B.T., Kieffer, B.L., Levitt, E.S., 2020. Differential impact of two critical respiratory centres in opioid-induced respiratory depression in awake mice. J. Physiol. 598, 189–205.
Von Euler, C., 1986. Brain stem mechanisms for generation and control of breathing pattern. In: Cherniack, N.S., Widdicombe, J.G. (Eds.), Handbook of Physiology. The Respiratory System. Control of Breathing. American Physiological Society, Bethesda, Maryland, pp. 1–67.
Von Euler, C., 1997. Neural organization and rhythm generation. In: Crystal, R.G., West, J.B., Barnes, P.J., Weibel, E.R. (Eds.), The Lung: Scientific Foundations, second edition ed. Lippincott-Raven, Philadelphia, pp. 1711–1724.
Wang, H., Germanson, T.P., Guyenet, P.G., 2002. Depressor and tachypneic responses to chemical stimulation of the ventral respiratory group are reduced by ablation of neurokinin-1 receptor-expressing neurons. J. Neurosci. 22, 3755–3764.
Yaksh, T.L., Woller, S.A., Ramachandran, R., Sorkin, L.S., 2015. The search for novel analgesics: targets and mechanisms. F1000Prime Rep. 7, 56.
Yang, C.F., Feldman, J.L., 2018. Efferent projections of excitatory and inhibitory preBötzinger Complex neurons. J. Comp. Neurol. 526, 1389–1402.
Yokota, S., Kaur, S., VanderHorst, V.G., Saper, C.B., Chamberlin, N.L., 2015. Respiratory-related outputs of glutamatergic, hypercapnia-responsive parabrachial neurons in mice. J. Comp. Neurol. 523, 907–920.
Zhang, Z., Xu, F., Zhang, C., Liang, X., 2007. Activation of opioid mu receptors in caudal medullary raphe region inhibits the ventilatory response to hypercapnia in anesthetized rats. Anesthesiology 107, 288–297.
Zhang, Z., Zhuang, J., Zhang, C., Xu, F., 2011. Activation of opioid mu-receptors in the commissural subdivision of the nucleus tractus solitarius abolishes the ventilatory response to hypoxia in anesthetized rats. Anesthesiology 115, 353–363.